NANO · MICRO small
www.small-journal.com

3D Cationic Polymeric Network Nanotrap for Efficient Collection of Perrhenate Anion from Wastewater

Xiaorui Li, Yiming Li, Huifang Wang, Zheng Niu, Yingjie He, Linfeng Jin, Mingyang Wu, Haiying Wang, Liyuan Chai,* Abdullah M. Al-Enizi, Ayman Nafady, Shoyebmohamad F. Shaikh, and Shengqian Ma**

Rhenium is one of the most valuable elements found in nature, and its capture and recycle are highly desirable for resource recovery. However, the effective and efficient collection of this material from industrial waste remains quite challenging. Herein, a tetraphenylmethane-based cationic polymeric network (CPN-tpm) nanotrap is designed, synthesized, and evaluated for ReO_4^- recovery. 3D building units are used to construct imidazolium salt-based polymers with positive charges, which yields a record maximum uptake capacity of 1133 mg g^{-1} for ReO_4^- collection as well as fast kinetics ReO_4^- uptake. The sorption equilibrium is reached within 20 min and a k_d value of 8.5×10^5 mL g^{-1} is obtained. The sorption capacity of CPN-tpm remains stable over a wide range of pH values and the removal efficiency exceeds 60% for pH levels below 2. Moreover, CPN-tpm exhibits good recyclability for at least five cycles of the sorption–desorption process. This work provides a new route for constructing a kind of new high-performance polymeric material for rhenium recovery and rhenium-contained industrial wastewater treatment.

1. Introduction

Rhenium (Re), as one of the most valuable and rare metal elements on planet earth, has been widely applied in aerospace and unleaded gasoline catalysis due to its excellent ductility and high melting point.[1] Currently, the annual worldwide production of rhenium is only 50 tons and the price remains extremely high, owing to the poor abundance of rhenium in the earth's crust and inexistence of monomineral in nature.[2] Nowadays, most of rhenium is produced from the wastewater of copper and molybdenum smelting process.[3] However, recovering rhenium efficiently and effectively remains quite challenging due to the complex conditions of the typical wastewater, such as acidic environment (pH range 1–5), low concentration of Re (lower than 40 mg L^{-1}), and large excess of competing anions (such as SO_4^{2-} and NO_3^-), and so on.[4] In the past decades, many efforts have been devoted to the recovery of rhenium and different methods (e.g., precipitation, adsorption, solvent extraction, and ion exchange[5]) have been developed. Among these methods, ion exchange represents one of the most promising methods for ReO_4^- capture and recovery, owing to its facile process, environmental benignity, and low cost.

In the past several years, various cationic materials have attracted considerable interest due to their utilization as the ion exchangers for ReO_4^- capture. Among these materials, the commercialized exchange resin PuroliteA-532E exhibited a good

X. Li, Y. He, Dr. L. Jin, M. Wu, Prof. H. Wang, Prof. L. Chai
School of Metallurgy and Environment
Central South University
Changsha, Hunan 410083, China
E-mail: haiyw25@csu.edu.cn; lychai@csu.edu.cn

X. Li, Prof. Y. Li
Department of Chemistry
University of South Florida
Tampa, FL 33620, USA

Prof. Y. Li
College of Chemistry and Chemical Engineering
Central South University
Changsha, Hunan 410083, China

Prof. H. Wang, Prof. Z. Niu
College of Chemistry
Chemical Engineering and Materials Science
Soochow University
Suzhou, Jiangsu 215123, China

Prof. H. Wang, Prof. L. Chai
Chinese National Engineering Research Center for Control & Treatment of Heavy Metal Pollution
Changsha, Hunan 410083, China

Prof. H. Wang
Water Pollution Control Technology Key Lab of Hunan Province
Changsha 410004, China

Prof. A. M. Al-Enizi, Prof. A. Nafady, S. F. Shaikh
Department of Chemistry
Collage of Science, King Saud University
Riyadh 11451, Saudi Arabia

Prof. S. Ma
Department of Chemistry
University of North Texas
Denton, TX 76201, USA
E-mail: shengqian.ma@unt.edu

The ORCID identification number(s) for the author(s) of this article can be found under https://doi.org/10.1002/smll.202007994.

DOI: 10.1002/smll.202007994

capacity but overly slow sorption kinetics.[6] Inorganic materials and composites were easily prepared at low cost, but the poor sorption capacity and slow kinetics hampered their further application.[6,7] For example, Shi and co-workers reported a Ti_2CT_x/PDDA nanocomposite with a Re(VII) removal capacity of 363 mg g^{-1} and equilibration in 1 h.[7d] Recently, considerable progress has been made for some cationic MOFs used for ReO_4^- capture; these materials exhibited good capacity and good selectivity. Wang and co-workers synthesized a series of MOFs for ReO_4^- uptake (as the surrogate for pertechnetate) with high selectivity.[8] However, the unstable feature of MOFs has limited their practical application in industry.[8,9] In recent years, cationic polymeric networks (CPNs) built by repeating organic building blocks with positive charges have been proposed as a promising material in different fields, including gas capture and separation,[10] anion exchange for pollution removal,[11] catalysis,[12] and antibacterial materials.[13] Compared with the traditional materials, CPNs have exhibited excellent features including facile synthesis process, controllable charge/pore size, good stability, and predictable functional structure for selective pollutants.[14] Porous ionic organic polymer PQA-Py-I, PQA-*p*NH_2Py-I, and PQA-*p*$N(Me)_2$Py-I with abundant quaternary ammonium were recently reported as materials for efficient ReO_4^- capture. PQA-*p*$N(Me)_2$Py-I exhibited the highest capacity ever reported and became the most promising material for the sorption toward ReO_4^-.[15]

To date, the reported high-performance cationic organic polymers for ReO_4^- capture is mainly based on the 1D and 2D building units, for example, tetraphenylethylene was considered as the planner quadrilateral building unit for forming 2D-unit-based CPNs,[14a,16]. Studies focused on 3D-building-unit-based ionic polymeric networks are rare. Owing to the rigid and shape-persistent tetrahedral structure with four connecting ends, tetraphenylmethane (tpm) has been widely used as a 3D building unit to construct amorphous networks and polymers in the past decades. Therefore, we employed tpm as the building unit to construct 3D-unit-based CPNs. An imidazolium group with positive charge played an essential role as the nanotrap for anion capture in the CPNs; while tpm, as a class of benzene-rich motif with high hydrophobicity provided high selectivity toward other anions in scavenging ReO_4^-.[8b,c,14d] This unique 3D building unit with high symmetry separated the positive charges uniformly and reduced the repulse from adjacent adsorbents. The higher rigidity of this unit (compared with that of other units) facilitates the ion-exchange process through the ion channels and yields larger absorption capacity.[17]

Herein, we report the synthesis of a tetraphenylmethane-based cationic polymeric network (CPN-tpm) and a study focused on its rapid and efficient uptake of perrhenate anion from water. CPN-tpm was synthesized through a solvothermal reaction with high yield (**Scheme 1**).[14a] Owing to the structure, CPN-tpm, a kind of 3D-unit-based cationic polymeric network, exhibited a maximum uptake capacity of 1133 mg g^{-1} for ReO_4^- capture and good recyclability for five repetitions of the sorption–desorption process. Furthermore, CPN-tpm exhibited fast ion exchange kinetics in 20 min, as evidenced by a k_d value 8.5×10^5 mL g^{-1}. The cationic polymeric network was stable even under strongly acidic solutions, consistent with the condition of most industrial wastewater. All these attributes indicated that the CPN-tpm material exhibits significant promise for perrhenate anion recovery from industrial wastewater.

CPN-tpm-Br was synthesized through a quaternization reaction between tetrakis[4-(1-imidazolyl)phenyl]methane (tipm) and 1,4-bis(bromomethyl)benzene in dimethylformamide (DMF) in a Schlenk tube. The synthetic route of CPN-tpm

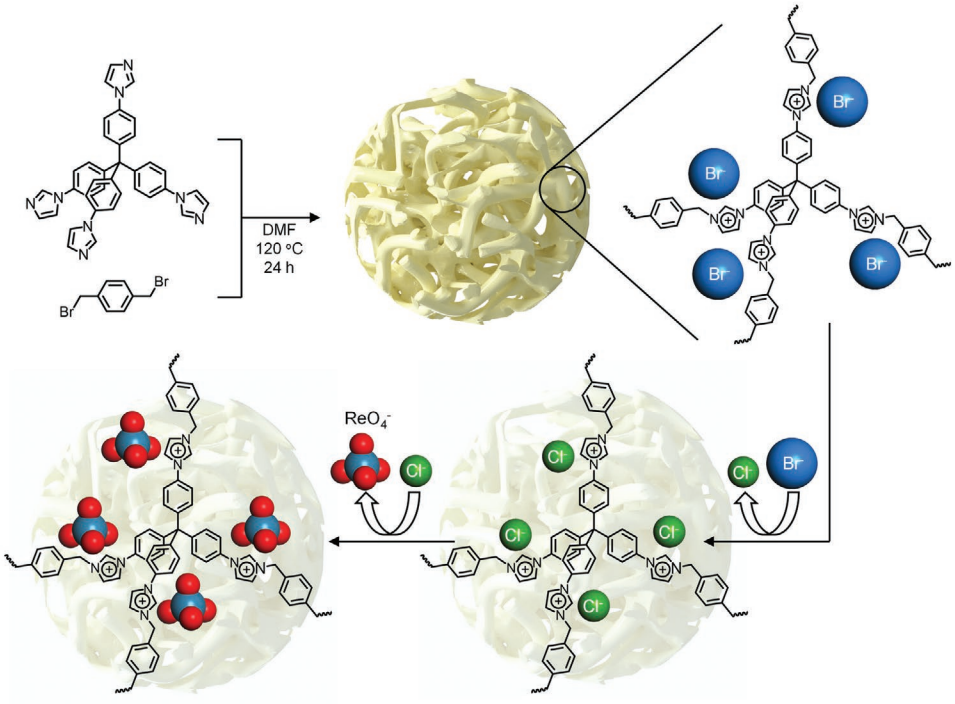

Scheme 1. Synthesis route of CPN-tpm and the anion-exchange process.

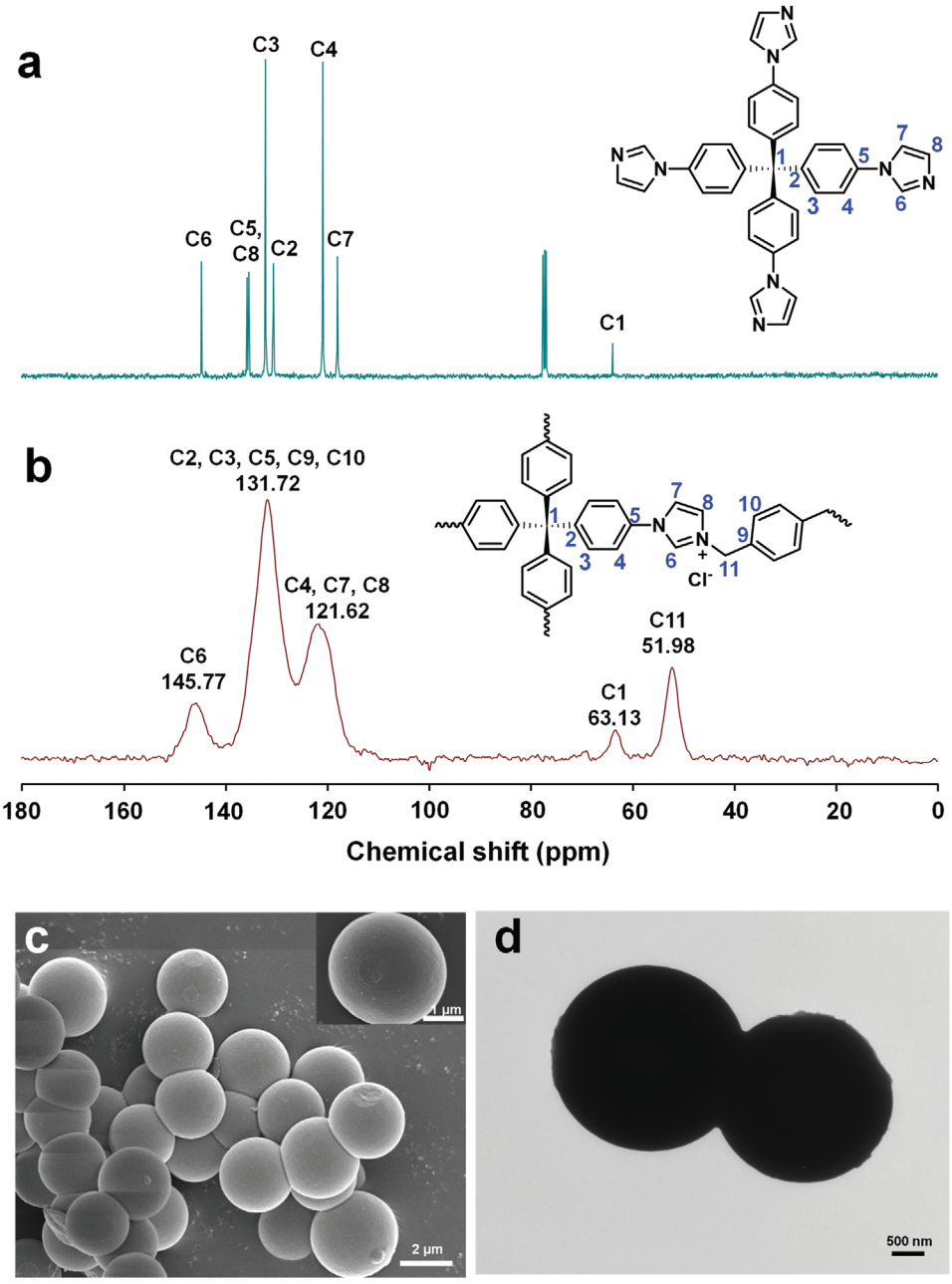

Figure 1. a) ^{13}C NMR (101 MHz, $CDCl_3$) spectrum of tipm; b) Solid-state ^{13}C NMR spectrum of CPN-tpm-Cl. c) SEM image of CPN-tpm-Br, particle size: ≈2 µm, scale bar = 2 µm, and inset scale bar = 1 µm. d) TEM image of CPN-tpm-Br, scale bar = 500 nm.

is shown in Scheme 1 (additional details can be found in the Supporting Information). 1,4-Bis(bromomethyl)benzene was used as a bridge between two different tipm building blocks to construct stable and robust polymeric networks with positive charges in the structure. Further soaking treatment of CPN-tpm-Br was performed for three times with sodium chloride solution, in order to obtain the cationic polymers with counter ion Cl^-. The resulting polymer was referred to as CPN-tpm-Cl.

To investigate the structure and morphology, the cationic polymeric networks were characterized by different techniques, including ^{13}C NMR, Fourier transform infrared (FT-IR) spectra, SEM, TEM, powder X-ray diffraction (PXRD) techniques, and thermogravimetric analysis (TGA). Solid-state ^{13}C NMR spectrum was used to confirm the successful synthesis of CPN-tpm-Cl. In order to assign the broad peaks of the networks, the ^{13}C NMR spectrum of the key precursor tipm was used as a comparison. As shown in **Figure 1a**,b, all the peaks corresponded to the relevant carbon atoms in the expected structure of tipm and CPN-tpm-Cl. The quaternization reaction was followed by a down-field shift of C8 in CPN-tpm-Cl to 121.62 ppm, in accordance with a previous study.[18] Furthermore, the characteristic peaks at 51.98 and 63.13 ppm (see Figure 1b) were attributed to

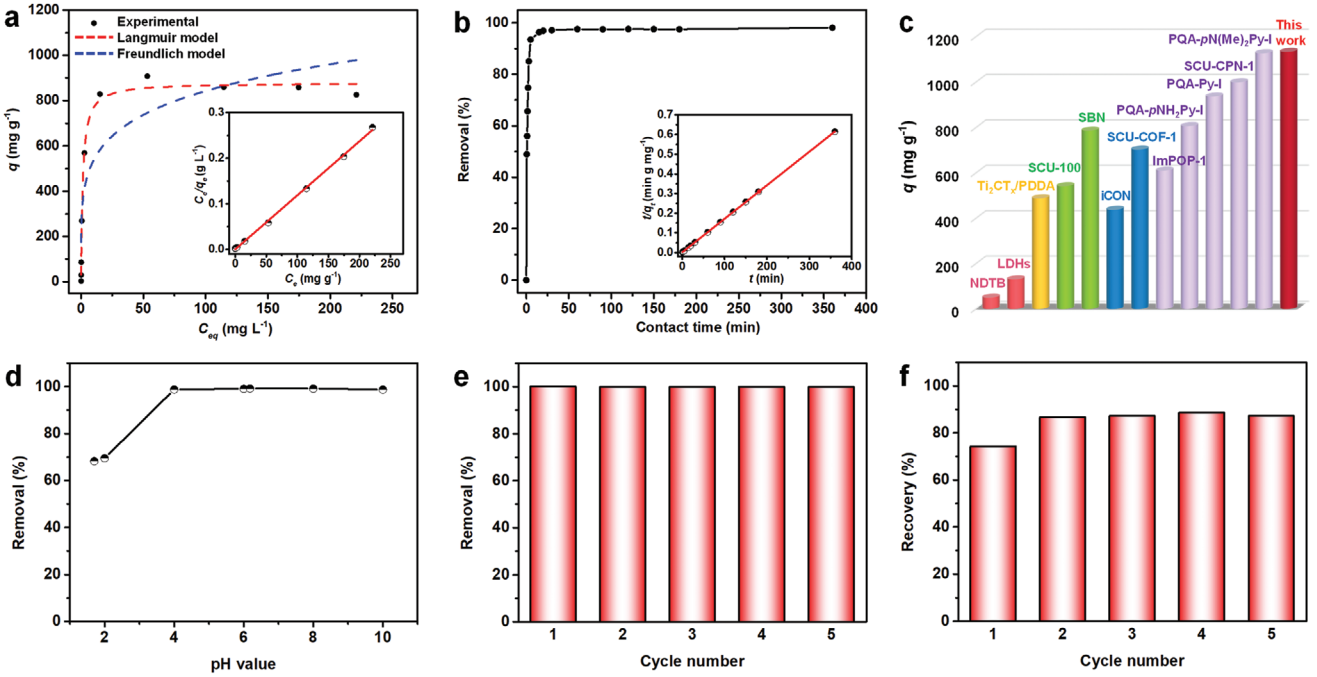

Figure 2. a) Sorption isotherm of CPN-tpm-Cl for ReO_4^- uptake, inset shows the fitting curve based on the Langmuir model. b) Sorption kinetics of CPN-tpm-Cl, inset shows the fitting curve based on the pseudo-second-order model. c) Sorption capacity of ReO_4^- from different materials (pink column: inorganic materials; yellow column: composites; green column: MOFs; blue column: COFs; purple column: polymers; red column: CPN-tpm-Cl in this work). d) Effect of pH on the sorption properties of ReO_4^- by CPN-tpm-Cl. Reversibility of CPN-tpm for e) collecting ReO_4^- and f) recycling ReO_4^-.

C11 (the sp^3-hybridized carbon atoms of methylene) and C1 (central carbon atoms), respectively. The peaks at 121.62 ppm (C4, C7, C8) and 145.77 ppm (C6) were attributed to the carbon atoms from the imidazolium rings and C4 from tetraphenylmethane, respectively.[19] Peaks occurring at 126–139 ppm resulted from carbons of different benzene rings (C2, C3, C5 and C9, C10).[14a,20] In addition, FT-IR spectra were used to further confirm the functional groups occurring in the structure. The characteristic peaks at 1074 cm^{-1} were assigned to quaternary imidazolium species, which resulted from the occurrence of the quaternization polymeric reaction, indicating the successful synthesis of CPN-tpm. Furthermore, scanning electron microscopy (SEM) and transmission electron microscopy (TEM) were performed to investigate the morphology of the polymer. CPN-tpm, a type of off-white powder (Figure S7, Supporting Information) on the macroscale, was characterized by full spherical morphology and a uniform particle distribution (particle diameter: ≈2 µm; see Figure 1c,d). The nitrogen adsorption–desorption isotherm of this amorphous material, as confirmed by means of PXRD measurements (Figure S8, Supporting Information), was collected at 77 K (Figure S9, Supporting Information). The result revealed negligible nitrogen uptake amount, suggesting that the pores of the CPN-tpm may be blocked by the counter ions and solvent molecules due to the positive charge on the skeleton.[14a] TGA was used to determine the thermal stability of CPN-tpm-Cl (Figure S10, Supporting Information). The result revealed an initial weight loss of ≈10% at temperatures below 150 °C, which may have been induced by the removal of water and DMF molecules. Similarly, CPN-tpm was stable up to 300 °C, demonstrating the good thermal stability of this material.

Given the predesigned architecture characterized by a combination of tetraphenylmethane backbone and cationic imidazolium units, the capacity of CPN-tpm for collecting perrhenate was studied. The sorption thermodynamics behavior was assessed from sorption isotherms of CPN-tpm-Cl for ReO_4^- obtained for initial ReO_4^- concentration ranging from 1 to 1000 ppm (**Figure 2a**). A Langmuir isotherm model (inset of Figure 2a) and Freundlich isotherm model (Figure S11, Supporting Information) were used to fit the data. The Langmuir isotherm model was better than the Freundlich isotherm model for describing the data, as evidenced by a high correlation coefficient ($R^2 > 0.99$). In addition, the calculated maximum sorption capacity based on the Langmuir isotherm model for ReO_4^-, 833.3 mg g^{-1} (Table S1, Supporting Information), is considerably lower than the experimental maximum sorption capacity of 1133 mg g^{-1} (see Table S4 (Supporting Information), and volumetric capacity was calculated as 723 mg cm^{-3}), owing to the excess ReO_4^- in the solution. Furthermore, the anion-exchange process was complete as we speculated, and (owing possibly to extra physical sorption) the theoretical maximum sorption capacity is 1073 mg g^{-1}, which was slightly lower than the experimental value. The sorption capacity obtained here is substantially higher than most of the values reported for the cationic materials, such as LDHs (130 mg g^{-1}), PuroliteA-532E (446 mg g^{-1}), SBN (786 mg g^{-1}), SLUG-21 (602 mg g^{-1}), SCU-100 (541 mg g^{-1}), SCU-COF-1 (702.4 mg g^{-1}), and ImPOP-1 (610 mg g^{-1}). Moreover, the value obtained here is even higher than the highest capacities ever reported (SCU-CPN-1 (999 mg g^{-1}) and PQA-*p*N$(Me)_2$Py-I (1127 mg g^{-1}, see Figure 2c and Table S3 (Supporting Information)). Compared with the

structure of 2D-unit-based CPNs in previous work, tipm as the 3D building unit further boosted the maximum uptake capacities of ReO_4^-. A removal percentage of over 99% was realized when the initial concentration and the equilibrium concentration of the residual Re in the solution were 30 ppm and 140 ppb, respectively. The results suggested that excellent sorption capacity toward ReO_4^- may be induced by the imidazolium moieties of CPN-tpm-Cl, which provide a positive charge for ion exchange between ReO_4^- and Cl^-.

The equilibrium time between adsorbents and anions was further investigated by evaluating the sorption kinetics. The experiments were conducted by collecting mixture at different times and separating these mixtures in preparation for Inductively coupled plasma optical emission spectrometry (ICP-OES) analysis. As shown in Figure 2b, the removal efficiency increased sharply to over 90% in the initial 5 min. The sorption equilibrium was reached within 20 min (96%), indicating a very fast sorption process. This process is considerably faster than those previously reported for various ionic materials, including PAF-1-F (24 h), SLUG-21 (48 h), UIO-66-NH_3^+ (24 h), PuroliteA-532E (150 min), NZVI/LDH (100 min), LDHs (>24 h), pFe (6 d), as shown in Table S3 in the Supporting Information. Such fast kinetics process will be beneficial when dealing with the industry wastewater. Pseudo-first-order (Figure S12, Supporting Information) and pseudo-second-order models (inset of Figure 2b) were applied to fit the data. The fitting results of the kinetic parameters are shown in Table S2 in the Supporting Information. The sorption kinetics of CPN-tpm-Cl toward ReO_4^- can be fitted with a pseudo-second-order model. Moreover, the high correlation coefficient ($R^2 > 0.9999$) realized indicates that the rate-determining step of the adsorption process between CPN-tpm-Cl and ReO_4^- may be chemical adsorption[14e,21]. As one of the most important indicators of sorbent effectiveness,[9c] the k_d value of CPN-tpm-Cl toward ReO_4^- was measured as 8.5×10^5 mL g^{-1}, which is among the highest values ever reported (Table S3, Supporting Information).

The effect of pH on the CPN-tpm-Cl removal efficiency of ReO_4^- was also studied to explore the applied pH range (from 1.7 to 10) under industrial conditions (liquid/solid ratio: 4000 mL g^{-1}). As shown in Figure 2d, the removal efficiency of ReO_4^- remained almost constant at 100% for pH ranging from 4 to 10. For pH values lower than 3, the efficiency decreased, owing to the excess Cl^- in the solution and its competition with ReO_4^-. The molar ratio between Cl^- and ReO_4^- reached levels of 250:1 and 25:1 at pH 1 and 2, respectively. Therefore, the high concentration of Cl^- can be used in the desorption process. At pH 1.7, a high ReO_4^- removal percentage of 68.2% was maintained, which is suitable for industrial wastewater with pH value close to 2 (Table S5, Supporting Information). To further investigate the reason for such high tolerance over a wide pH range, a Zeta Potential test was conducted in solution at different pH values.[22] The results (Figure S13, Supporting Information) that CPN-tpm exhibited positive values over a wide range of pH (1 to 11), indicating that the surface of CPN-tpm was positively charged and was effective in capturing anionic pollutions in a wide pH range.[23] Moreover, as one of the most essential properties of adsorbents in industry, the recyclability of CPN-tpm was also evaluated. After four cycles of the regeneration process with 2 M NaCl solution, the sorption performance of CPN-tpm-Cl still remained almost unchanged (at 99.7%) in the last run (Figure 2e). The recovery efficiency of CPN-tpm-Cl was almost over 85% (see Figure 2f), except in the first run (74%), owing possibly to the nearly complete desorption that occurred during the process of recovery. With such broad range of tolerated pH and good regeneration, CPN-tpm exhibits significant promise for ReO_4^- collection from industrial waste.

Selectivity is another essential factor for identifying a promising candidate for anion collection. A high concentration of SO_4^{2-} and arsenicum-contained anions in industrial wastewater (data from a certain copper smelting plant in southern China, shown in Table S5 in the Supporting Information) as well as a high concentration of NO_3^- ions in nuclear wastewater must be taken into consideration.[24] Therefore, SO_4^{2-}, AsO_4^{3-}, and NO_3^- were selected for investigating the sorption selectivity considering different ion configurations and different charge densities compared with those of ReO_4^-. As shown in **Figure 3a**, when the molar ratios of NO_3^-, SO_4^{2-}, and AsO_4^{3-} were ten times in excess in the Re-contained solution, the corresponding removal efficiencies for ReO_4^- were 98.6%, 91.3%, and 82.06%, respectively (solid to liquid ratio of CPN-tpm-Cl: 1000 mL g^{-1}). The high selectivity results probably from the strong affinity between the perrhenate anion with low charge density and the 3D hydrophobic skeleton with positive charges.[8c,14d] And a series of concentrations for each competing anion were studied to account for the different concentrations in the industrial wastewater. A removal efficiency of 49.1% was realized for a SO_4^{2-} ion molar ratio of 5000 times. In addition, 29.4% of ReO_4^- ions was captured from a solution of 0.16×10^{-3} M ReO_4^- and 160×10^{-3} M NO_3^-. We attributed the reduction to the dynamic ion-exchange process between the ReO_4^- ions and competing anions in large

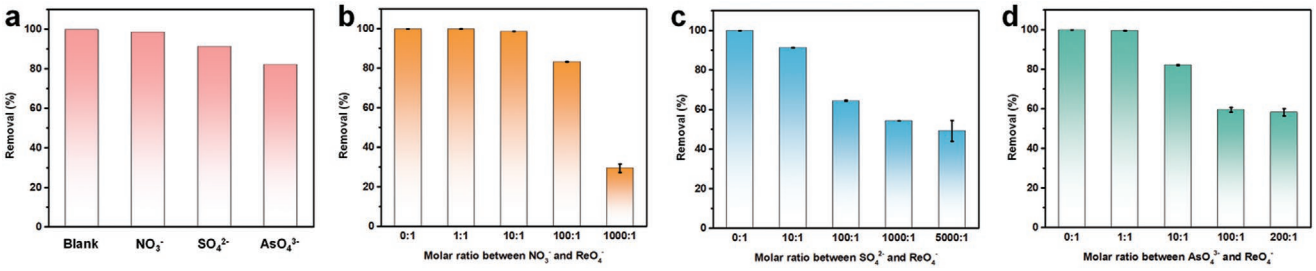

Figure 3. a) Effect of typical competing anions (1.6×10^{-3} M) on the removal percentage of ReO_4^- (initial concentration of ReO_4^- : 0.16×10^{-3} M). b–d) Effect of competing NO_3^- anions, competing SO_4^{2-} anions, and competing AsO_4^{3-} anions, respectively, on the anion-exchange of ReO_4^- by CPN-tpm-Cl.

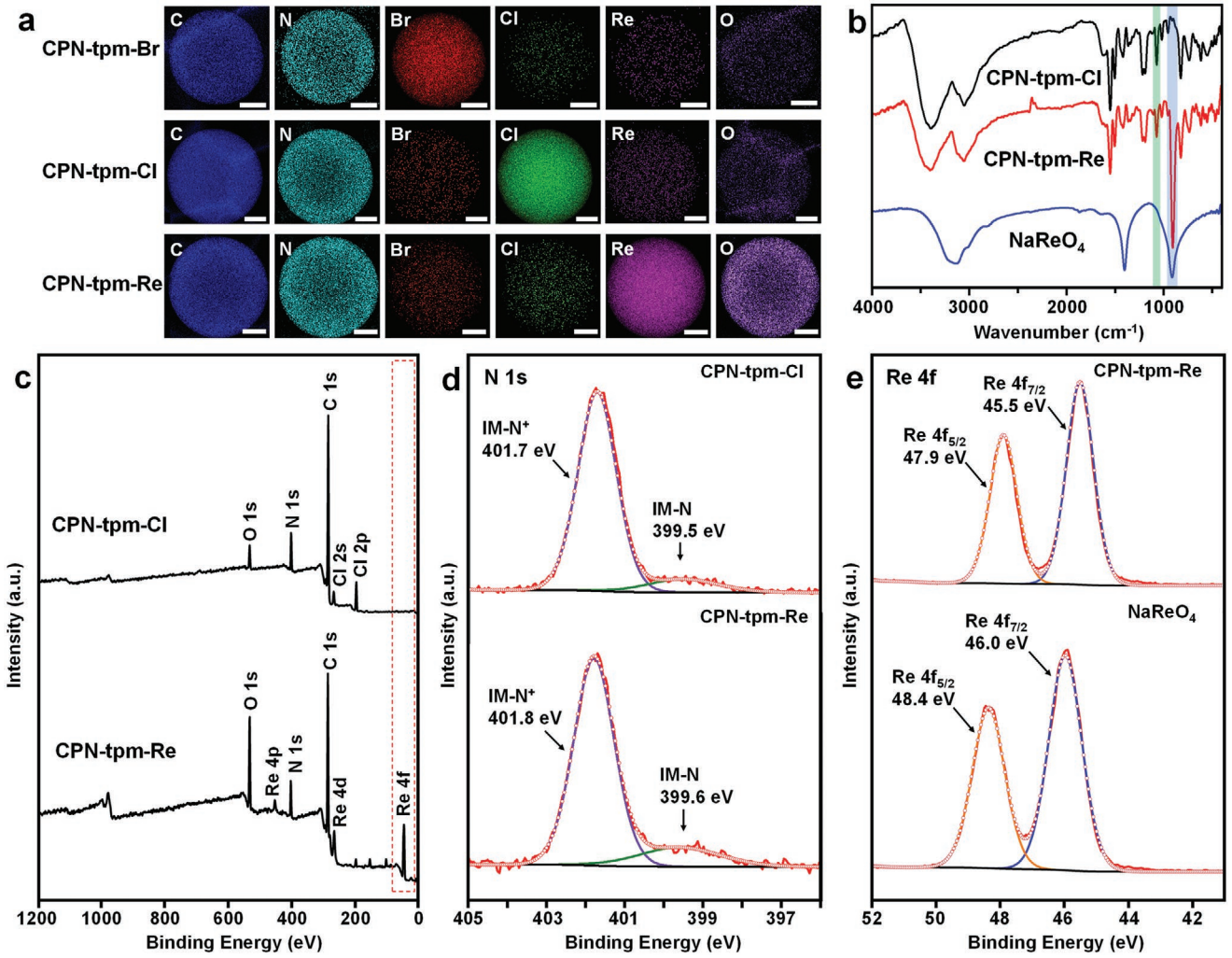

Figure 4. a) TEM-EDS mapping of CPN-tpm-Br, CPN-tpm-Cl, and CPN-tpm-Re, qualitatively indicative of the anion-exchange process, scale bar = 700 nm. b) FT-IR spectra of CPN-tpm before and after anion-exchange with ReO_4^- and $NaReO_4$. Characteristics peaks occurring at 1074 cm^{-1} (green band) and 902 cm^{-1} (blue band) corresponded to the quaternary imidazolium species and ReO_4^-, respectively. c) XPS survey spectra of CPN-tpm-Cl and CPN-tpm-Re. d) N 1s core-level spectra of CPN-tpm-Cl and CPN-tpm-Re. e) XPS analysis of Re 4f from ReO_4^- sorbed CPN-tpm and $NaReO_4$.

excess. Wang and co-workers performed DFT theoretical studies involving the ReO_4^- anion.[14a] The results revealed that the interaction between NO_3^- and the cationic imidazole group is a "corner-to-corner" type, while the imidazole ring with ReO_4^- exhibited a more stable "face-to-face" stacking structure, leading to a higher binding energy between the polymer and ReO_4^-. These results suggested that the imidazole ring with positive charge plays an essential role in the selective uptake of ReO_4^- over NO_3^-, SO_4^{2-}, AsO_4^{3-}, and other competing anions. Thus, by incorporating such imidazolium rings, CPN-tpm kept the advantages of high selectivity and can be considered a competent candidate for ReO_4^- capture from industrial wastewater.

The anion exchange process of CPN-tpm was studied further using techniques such as TEM-EDS mapping, FT-IR, and X-ray photoelectron spectroscopy (XPS) analysis. As shown in **Figure 4c**, compared with the XPS survey spectrum of CPN-tpm-Cl, the spectrum of CPN-tpm-Re consisted of Re 4f (46 eV), Re 4d (265 eV), and Re 4p (452 eV) peaks. This indicated that the Re species adsorbed on the surface of the CPN-tpm after the sorption experiments.[25] The Re 4f core-level spectra of CPN-tpm-Re (Figure 4e) showed that the oxidation state of Re species on the surface of the material was Re(VII).[14d] Furthermore, the peak at 902 cm^{-1} in the FT-IR spectrum of CPN-tpm-Re can be attributed to Re-O ν_3 asymmetric stretching (Figure 4b), indicating the presence of ReO_4^- after adsorption.[14a] Moreover, a 0.5 eV binding energy shift from 46.0 eV ($NaReO_4$) to 45.5 eV (CPN-tpm-Re), owing to the increase in electron density induced mainly by the interaction with the polymer, was observed for the Re 4f signal.[14d] This suggested that the Re species existed as ReO_4^- for interaction with the cationic skeleton. To further verify the binding behavior of ReO_4^- with CPN-tpm, the N 1s core-level spectra of CPN-tpm-Cl and CPN-tpm-Re were analyzed. The spectra (Figure 4d) revealed different types of N-containing functional groups, the nonionic N atoms in imidazole ring (IM-N) and N atoms in imidazolium ($IM\text{-}N^+$). After the adsorption, these binding energies increased from 399.5 and 401.7 eV (CPN-tpm-Cl) to 399.6 and 401.8 eV (CPN-tpm-Re), respectively.[19] These changes suggested that a strong

interaction occurred between the cationic N-containing polymeric skeleton and negatively charged ReO_4^-. This may have resulted from the larger ionic radius and lower charge density of ReO_4^- compared with those of Cl^- (radius of ReO_4^-: 0.260 nm and radius of Cl^-: 0.172 nm).[26] The peak corresponding to Cl species at a binding energy of 197 eV was barely observed in the XPS survey scan spectrum (Figure 4c). However, the peaks at 196.8 and 198.4 eV in the Cl 2p core-level spectra of CPN-tpm-Cl were related to Cl^- (see Figure S14 in the Supporting Information), indicating that Cl^- played an important role in the ion-exchange process. This finding was consistent with the results obtained from TEM-EDS mapping of CPN-tpm-Br, CPN-tpm-Cl, and CPN-tpm-Re (Figure 4a). The TEM-EDS mapping images of CPN-tpm before and after ReO_4^- sorption showed that the distribution of Cl element and Br element decreased and the distribution of Re element increased significantly in CPN-tpm-Re. The complete anion-exchange process can be confirmed by means of SEM-EDS analysis (Figure S15, Supporting Information). From Figure S16 (Supporting Information), we can see that ion-exchange process from Cl^- to ReO_4^- was facile and could maintain the morphology of the polymeric network. Thus, the sorption mechanism of CPN-tpm for ReO_4^- occurred via the ion-exchange process between Cl^- and ReO_4^-, which was induced by electrostatic attraction between the cationic imidazolium group and the ReO_4^- anion.

To explain the super-high ReO_4^- uptake capacity, the function of the tpm motif was further studied via DFT theoretical studies. The high uptake selectivity and capacity of ReO_4^- induced by the imidazolium ring were investigated by means of DFT calculations in previous work.[14a] In this work, we highlight the higher capacity of CPN-tpm constructed by 3D building units of tipm (relative to that resulting from 2D building units), through comparison of different benzene-rich backbone structures. To reveal the basis for this higher capacity, we compared the binding energies of ReO_4^- with those of two model systems, i.e., CPN-tpm presented in this work and SCU-CPN-1 constructed by 2D building units. The fragment, $[Ph_2\text{-}C\text{-}(C_6H_5\text{–}C_3N_2H_3\text{–}CH_2\text{–}C_6H_5)_2]^{2+}$ (referred to as L^{2+} hereafter), was built as a model for mimicking the critical local structure of the amorphous sorbent CPN-tpm material in the present work (see **Figure 5a**). The other, $[Ph_2\text{-}C{=}C\text{-}(C_6H_5\text{–}C_3N_2H_3\text{–}CH_2\text{–}C_6H_5)_2]^{2+}$ (referred to as M^{2+} hereafter), was built as a model for SCU-CPN-1 described in Wang's work.[14a] The calculated binding energy of $L^{2+}(ReO_4^-)_2$, i.e., –15.5 kcal mol^{-1}, is 3.1 kcal mol^{-1} higher than that of $M^{2+}(ReO_4^-)_2$ (–12.4 kcal mol^{-1}). This indicated that the binding energy of each ReO_4^- with CPN-tpm is (on average) ≈1.5 kcal mol^{-1} higher than that of SCU-CPN-1. Moreover, the distance between two ReO_4^- anions in the $M^{2+}(ReO_4^-)_2$ complex is shorter than that in the $L^{2+}(ReO_4^-)_2$ complex (5.86 vs 7.47 Å). The cross-section of the electrostatic potential map (ESP) shown in Figure 5b shows that the repulsive electrostatic interaction between the two ReO_4^- anions in the $M^{2+}(ReO_4^-)_2$ complex is greater than that in the $L^{2+}(ReO_4^-)_2$ complex. This may have resulted in the higher binding energy of ReO_4^- with L^{2+} (than with M^{2+}) and the improved ReO_4^- adsorption in CPN-tpm. Therefore, modification of the planar C=C to a tetrahedral C atom in tpm-based polymeric networks would separate the positive charges uniformly in limit interspace and reduce the repulsive interaction between two adjacent ReO_4^- adsorbents. This would lead to an increase in the ReO_4^- uptake amount. In addition, the positively charged imidazolium rings and the tetrahedral ReO_4^- anions could form a face-to-face stacking structure with a higher binding energy (than that of other structures; the high uptake selectivity for ReO_4^- has been discussed by Wang and co-workers).[14a] This indicated that the CPN-tpm-Cl has maintained the advantages of the rings with high selectivity of ReO_4^-, and further improved the uptake capacity by employing 3D building units. CPN-tpm-Cl is therefore a promising candidate for use in real circumstances involving the industry wastewater.

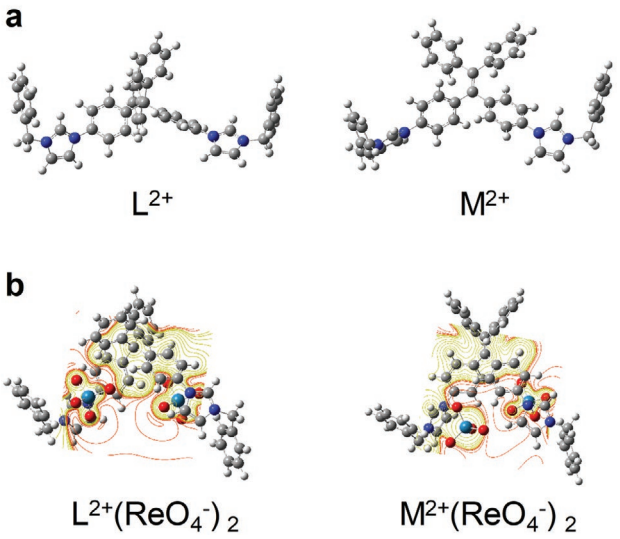

Figure 5. a) Structure of L^{2+} ($[Ph_2\text{-}C\text{-}(C_6H_5\text{–}C_3N_2H_3\text{–}CH_2\text{–}C_6H_5)_2]^{2+}$ fragment) (left) and M^{2+} ($[Ph_2\text{-}C{=}C\text{-}(C_6H_5\text{–}C_3N_2H_3\text{–}CH_2\text{–}C_6H_5)_2]^{2+}$ fragment) (right). b) Electrostatic potential map (ESP) obtained for the cross-section of complexes $L^{2+}(ReO_4^-)_2$ (left) and $M^{2+}(ReO_4^-)_2$ (right).

2. Conclusion

In summary, based on the structure-property correlation design, we have successfully synthesized a cationic polymeric network nanotrap CPN-tpm based on 3D building units. Benefiting from the highly symmetric structure and strong rigidity from the tetrahedral tpm building unit, the positive charges from imidazolium were uniformly distributed and the repulse from adjacent cations was reduced. This led to a significant enhancement of the adsorption performance. An uptake capacity of 1133 mg g^{-1} for ReO_4^- collection, which is the highest ever reported, was measured for this positively charged material exhibited. Furthermore, the material was characterized by high uptake capacity, fast kinetics, good selectivity, and excellent recyclability, and represents a promising ion exchange material for rhenium recovery from industrial waste.

Supporting Information

Supporting Information is available from the Wiley Online Library or from the author.

Acknowledgements

The authors acknowledge the financial support received from the key project of National Natural Science Foundation of China (51634010), National Science Fund for Distinguished Young Scholars (51825403), National Key R&D Program of China (2020YFC1909204), Key R&D Program of Hunan Province (2018SK2026), China Scholarship Council (CSC) (201706370186). Partial financial support from the US National Science Foundation (CBET-1706025) and the Robert A. Welch Foundation (B-0027) is also acknowledged (S.M.). The authors also extended their sincere appreciation to Researchers Supporting Program project no (RSP-2021/55) at King Saud University, Riyadh, Saudi Arabia for funding this work (A.M.A. and A.N.).

Conflict of Interest

The authors declare no conflict of interest.

Data Availability Statement

The data that support the findings of this study are available on request from the corresponding author. The data are not publicly available due to privacy or ethical restrictions.

Keywords

3D building units, cationic polymeric networks, ion exchange, nanotrap, perrhenate anions

Received: December 20, 2020
Revised: February 18, 2021
Published online: March 21, 2021

[1] a) C. D. Anderson, P. R. Taylor, C. G. Anderson, *Miner. Metall. Proc.* **2013**, *30*, 59; b) A. N. Zagorodnyaya, Z. S. Abisheva, L. Y. Agapova, A. S. Sharipova, *Theor. Found. Chem. Eng.* **2019**, *53*, 841.

[2] a) A. G. Kholmogorov, O. N. Kononova, S. V. Kachin, S. N. Ilyichev, V. V. Kryuchkov, O. P. Kalyakina, G. L. Pashkov, *Hydrometallurgy* **1999**, *51*, 19; b) D. Bernhardt, J. F. Reilly, *Mineral Commodity Summaries 2019*, U.S. Geological Survey, Reston, VA **2019**; c) H. S. Kim, J. S. Park, S. Y. Seo, T. Tran, M. J. Kim, *Hydrometallurgy* **2015**, *156*, 158.

[3] D.-w. Fang, W.-j. Shan, Q. Yan, D. Li, L.-x. Xia, S.-l. Zang, *Fluid Phase Equilib.* **2014**, *383*, 1.

[4] a) B. Zhang, H.-Z. Liu, W. Wang, Z.-G. Gao, Y.-H. Cao, *Hydrometallurgy* **2017**, *173*, 50; b) N. Nebeker, J. B. Hiskey, *Hydrometallurgy* **2012**, *125–126*, 64.

[5] Y. Huang, H. Hu, *Chem. Eng. J.* **2020**, *381*, 122647.

[6] L. Zhu, C. L. Xiao, X. Dai, J. Li, D. X. Gui, D. P. Sheng, L. H. Chen, R. H. Zhou, Z. F. Chai, T. E. Albrecht-Schmitt, S. Wang, *Environ. Sci. Technol. Lett.* **2017**, *4*, 316.

[7] a) D. Li, J. C. Seaman, S. E. Hunyadi Murph, D. I. Kaplan, K. Taylor-Pashow, R. Feng, H. Chang, M. Tandukar, *J. Hazard. Mater.* **2019**, *374*, 177; b) G. Sheng, Y. Tang, W. Linghu, L. Wang, J. Li, H. Li, X. Wang, Y. Huang, *Appl. Catal., B* **2016**, *192*, 268; c) H. Hu, L. Sun, Y. Gao, T. Wang, Y. Huang, C. Lv, Y. F. Zhang, Q. Huang, X. Chen, H. Wu, *J. Hazard. Mater.* **2019**, *387*, 121670; d) L. Wang, H. Song, L. Yuan, Z. Li, P. Zhang, J. K. Gibson, L. Zheng, H. Wang, Z. Chai, W. Shi, *Environ. Sci. Technol.* **2019**, *53*, 3739.

[8] a) D. P. Sheng, L. Zhu, C. Xu, C. L. Xiao, Y. L. Wang, Y. X. Wang, L. H. Chen, J. Diwu, J. Chen, Z. F. Chai, T. E. Albrecht-Schmitt, S. A. Wang, *Environ. Sci. Technol.* **2017**, *51*, 3471; b) D. Sheng, L. Zhu, X. Dai, C. Xu, P. Li, C. Pearce, C. Xiao, J. Chen, R. Zhou, T. Duan, O. K. Farha, Z. Chai, S. Wang, *Angew. Chem., Int. Ed.* **2019**, *58*, 4968; c) L. Zhu, D. P. Sheng, C. Xu, X. Dai, M. A. Silver, J. Li, P. Li, Y. X. Wang, Y. L. Wang, L. H. Chen, C. L. Xiao, J. Chen, R. H. Zhou, C. Zhang, O. K. Farha, Z. F. Chai, T. E. Albrecht-Schmitt, S. Wang, *J. Am. Chem. Soc.* **2017**, *139*, 14873.

[9] a) D. Banerjee, W. Q. Xu, Z. M. Nie, L. E. V. Johnson, C. Coghlan, M. L. Sushko, D. Kim, M. J. Schweiger, A. A. Kruger, C. J. Doonan, P. K. Thallapally, *Inorg. Chem.* **2016**, *55*, 8241; b) H. H. Fei, M. R. Bresler, S. R. J. Oliver, *J. Am. Chem. Soc.* **2011**, *133*, 11110; c) C. P. Li, J. Y. Ai, H. Zhou, Q. Chen, Y. Yang, H. He, M. Du, *Chem. Commun.* **2019**, *55*, 1841; d) E. Soe, B. Ehlke, S. R. J. Oliver, *Environ. Sci. Technol.* **2019**, *53*, 7663.

[10] S. Fischer, A. Schimanowitz, R. Dawson, I. Senkovska, S. Kaskel, A. Thomas, *J. Mater. Chem. A* **2014**, *2*, 11825.

[11] Y. Q. Su, Y. X. Wang, X. J. Li, X. X. Li, R. H. Wang, *ACS Appl. Mater. Interfaces* **2016**, *8*, 18904.

[12] a) J. Li, D. Jia, Z. Guo, Y. Liu, Y. Lyu, Y. Zhou, J. Wang, *Green Chem.* **2017**, *19*, 2675; b) Q. Sun, S. Ma, Z. Dai, X. Meng, F.-S. Xiao, *J. Mater. Chem. A* **2015**, *3*, 23871; c) O. Buyukcakir, S. H. Je, D. S. Choi, S. N. Talapaneni, Y. Seo, Y. Jung, K. Polychronopoulou, A. Coskun, *Chem. Commun.* **2016**, *52*, 934; d) T. T. Liu, R. Xu, J. D. Yi, J. Liang, X. S. Wang, P. C. Shi, Y. B. Huang, R. Cao, *ChemCatChem* **2018**, *10*, 2036.

[13] Y. Yuan, F. Sun, F. Zhang, H. Ren, M. Guo, K. Cai, X. Jing, X. Gao, G. Zhu, *Adv. Mater.* **2013**, *25*, 6619.

[14] a) J. Li, X. Dai, L. Zhu, C. Xu, D. Zhang, M. A. Silver, P. Li, L. H. Chen, Y. Z. Li, D. W. Zuo, H. Zhang, C. L. Xiao, J. Chen, J. Diwu, O. K. Farha, T. E. Albrecht-Schmitt, Z. F. Chai, S. A. Wang, *Nat. Commun.* **2018**, *9*, 3007; b) J. Shen, W. Chai, K. X. Wang, F. Zhang, *ACS Appl. Mater. Interfaces* **2017**, *9*, 22440; c) D. Banerjee, S. K. Elsaidi, B. Aguila, B. Y. Li, D. Kim, M. J. Schweiger, A. A. Kruger, C. J. Doonan, S. Q. Ma, P. K. Thallapally, *Chem. - Eur. J.* **2016**, *22*, 17581; d) Z. W. Liu, B. H. Han, *Environ. Sci. Technol.* **2020**, *54*, 216; e) M. Ding, L. Chen, Y. Xu, B. Chen, J. Ding, R. Wu, C. Huang, Y. He, Y. Jin, C. Xia, *Chem. Eng. J.* **2020**, *380*, 122581.

[15] Q. Sun, L. Zhu, B. Aguila, P. K. Thallapally, C. Xu, J. Chen, S. Wang, D. Rogers, S. Ma, *Nat. Commun.* **2019**, *10*, 1646.

[16] F. Beuerle, B. Gole, *Angew. Chem., Int. Ed.* **2018**, *57*, 4850.

[17] a) T. Li, W. Zhu, R. Shen, H.-Y. Wang, W. Chen, S.-J. Hao, Y. Li, Z.-G. Gu, Z. Li, *New J. Chem.* **2018**, *42*, 6247; b) X. Hu, H. Wang, C. F. J. Faul, J. Wen, Y. Wei, M. Zhu, Y. Liao, *Chem. Eng. J.* **2020**, *382*, 122998.

[18] J. Alcázar, A. De la Hoz, M. J. M. r. i. c. Begtrup, *Magn. Reson. Chem.* **1998**, *36*, 296.

[19] Y. Zhang, G. Chen, L. Wu, K. Liu, H. Zhong, Z. Long, M. Tong, Z. Yang, S. Dai, *Chem. Commun.* **2020**, *56*, 3309.

[20] a) M. Lin, S. Wang, J. Zhang, W. Luo, H. Liu, W. Wang, C.-Y. Su, *J. Mol. Catal. A: Chem.* **2014**, *394*, 33; b) J. Choi, H. Y. Yang, H. J. Kim, S. U. Son, *Angew. Chem., Int. Ed.* **2010**, *49*, 7718.

[21] W. Tao, H. Zhong, X. Pan, P. Wang, H. Wang, L. Huang, *J. Hazard. Mater.* **2020**, *384*, 121373.

[22] H. Wang, H. Deng, Y. He, L. Huang, D. Wei, T. Hao, S. Wang, L. Jin, L. Zhang, *Chem. Eng. J.* **2020**, *396*, 125249.

[23] Y. Xie, J. Lin, H. Lin, Y. Jiang, J. Liang, H. Wang, S. Tu, J. Li, *J. Hazard. Mater.* **2020**, *392*, 122496.

[24] a) L. He, S. Liu, L. Chen, X. Dai, J. Li, M. Zhang, F. Ma, C. Zhang, Z. Yang, R. Zhou, Z. Chai, S. Wang, *Chem. Sci.* **2019**, *10*, 4293; b) Z. S. Abisheva, A. N. Zagorodnyaya, N. S. Bekturganov, *Hydrometallurgy* **2011**, *109*, 1.

[25] Z. Guo, M. Shams, C. Zhu, Q. Shi, Y. Tian, M. H. Engelhard, D. Du, I. Chowdhury, Y. Lin, *Environ. Sci. Technol.* **2019**, *53*, 2612.

[26] a) I. J. Villar-Garcia, E. F. Smith, A. W. Taylor, F. Qiu, K. R. Lovelock, R. G. Jones, P. Licence, *Phys. Chem. Chem. Phys.* **2011**, *13*, 2797; b) H. J. Da, C. X. Yang, X. P. Yan, *Environ. Sci. Technol.* **2019**, *53*, 5212.

